A polyethylene glycol functionalized hyaluronic acid coating for cardiovascular catheter lubrication

Sharma, Prashant; Wan, Hongping; Lin, Chengxiong; Kaper, Hans J.

Published in:
Materials & design

DOI:
10.1016/j.matdes.2020.109080

Publication date:
2020

Materials and Design 196 (2020) 109080

Contents lists available at ScienceDirect

Materials and Design

journal homepage: www.elsevier.com/locate/matdes

A polyethylene glycol functionalized hyaluronic acid coating for cardiovascular catheter lubrication

Hongping Wan [1], Chengxiong Lin [1], Hans J. Kaper, Prashant K. Sharma *

University of Groningen and University Medical Center Groningen, Department of Biomedical Engineering, Groningen, the Netherlands.

HIGHLIGHTS

- The catheter-blood vessel sliding interface was successfully mimicked using a reciprocating aorta- PU (polyurethane) ballfrictional system.
- An ultra-thin, lubricant, and biocompatible coating based on two biopolymers was successfully fabricated.
- The coating significantly improved the lubrication of polyurethane and prevented the wear of blood vessel.
- The HADN-PBA thus is a strong candidate for cardiovascular catheter coating.

GRAPHICAL ABSTRACT

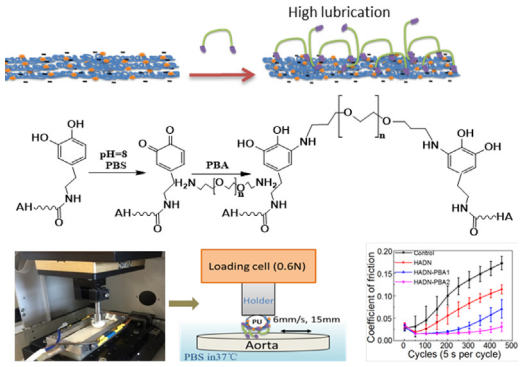

ARTICLE INFO

Article history:
Received 30 June 2020
Received in revised form 18 August 2020
Accepted 19 August 2020
Available online 21 August 2020

Keywords:
HADN-PBA coating
Aorta
Friction
Energy dissipation

ABSTRACT

Catheterization is a common medical operation for cardiovascular disease diagnosis and treatment, where low friction is attained through hydrophilic lubricious coatings. But these coatings can cause iatrogenic complications when particles become lose and float freely in the blood stream. Here we present an ultra-thin coating based on polyethylene glycol (PEG) functionalized hyaluronic acid (HA). The mussel-inspired biopolymer hyaluronic acid was first conjugated to dopamine (DN) to get HADN and then poly (ethylene glycol) bis (3-amino-propyl) terminated (PBA) was used to functionalize the HADN with PEG. The reciprocating sliding ball-on-flat ex vivo model based on PU ball and porcine aorta was used to evaluate the lubrication performance and the results suggest coating of HADN with best lubrication enhancement. After 40 min friction test, the surface of aorta remained intact for HADN-PBA coated PU as compared to HADN coating and positive control (sliding against bare PU). The amount of glycocalyx, number of endothelial nuclei and intima surface of aorta for coated PU were similar to negative control (without rubbing). Besides lubrication, the high biocompatibility suggests the coating of HADN-PBA is safe and lubrication benefits to the cardiovascular catheter.

1. Introduction

The function of many medical device and implant in biological systems depends on appropriate lubrication at the sliding interface. Cardiovascular catheterization, for instance, is a procedure where a catheter slides through the blood vessels for about a meter to the heart in order to diagnose and treat cardiovascular diseases. During the procedure, friction and wear naturally occurs between catheter and blood vessel which can induce vasoconstriction and injury leading to intimal proliferation or distal embolization associated with wear of organ and infarction [1]. It is estimated that 25% of all hospitalized patients received intravenous infusions and that there are a growing number of outpatients that require frequent catheterization [2]. Catheters

* Corresponding author.
E-mail address: p.k.sharma@umcg.nl (P.K. Sharma).
[1]Hongping Wan and Chengxiong Lin have contributed equally in this paper and share the first author.

https://doi.org/10.1016/j.matdes.2020.109080

are directly in contact with biological fluids such as blood or urine during intervention [3] and the friction between catheter and tissue may induce vasoconstriction and vessel wall injury [4,5].

To maintain safe catheterization, hydrophilic and highly lubrication coatings are used clinically for the catheters, although recently many reports warned the scientific community of the iatrogenic complications due to particulate release in the blood stream causing embolization [6,7] with further ramifications [8–11]. Surface modification technology [12–16] to develop thin (non-swelling) coatings has been used to improve the tribological performance of device and catheter for some time. Ho et al. [17] reported a coating of poly (2-methacryloyloxyethyl phosphorylcholine-*co*-n-butyl methacrylate [poly(MPC-*co*-BMA)] on PU surface yield a least friction due to the sufficient hydration and boundary lubrication enable by the polymer. The tribological and chemical characteristics of poly(MPC-*co*-BMA) increased the efficacy of PU for clinical applications. However these studies mainly focus on the physical-chemical properties of the structure of materials itself rather than the real tissue. As a result, the effect of lubrication between coating and tissue remains unclear, which is quite important for clinical application. An effective catheter coating required high adhesivity to the catheter surface (often poly-urethane, PU) on one side to avoid spalling and delamination, and high lubricity along with biocompatibility on the other side. Thus the aim of this study is to modify PU surface with an ultra-thin, stable and high biocompatibility coating to enhance sliding lubrication against blood vessel lumen.

Biomacromolecules like proteins, glycoproteins and polysaccharides support a wide range of normal and shear stresses [18] at sliding interfaces [19]. Effective lubricants including various hydrophilic, zwitterionic and high-molecular weight biopolymer such as glycoproteins, lipids [20] and hyaluronic acid (HA) [21], which work synergistically to support a wide range of normal and shear stresses [18]. Due to their chemical structure, and conformation these macromolecules provide extremely low friction and protection against wear of the surrounding tissue. Hyaluronic acid (HA), the major compound in synovial fluid and tear film [21–23], provides the effective lubrication in the articular joint, while it does not easily adsorb to surface by its self. In this respect, 3,4-dihydroxy-*L*-phenylalanine (DOPA), whose ortho-dihydroxyphenyl (catechol) group is characterized of widely adhesive on various inorganic/organic surfaces [24] and can be readily coupled to the carboxyl residues on HA via carbodiimide chemistry [25,26]. Dopamine conjugated HA (HADN) is adhesive in nature and have been used in the past for increasing cell responsive [26] showing a great potential in biomedical application. In our study HADN is important to adhere to the hydrophobic PU surface and give rise to high cohesive strength of the HADN layer on the PU surface. Polyethylene glycol (PEG) as an artificial lubricant for prevention of wear have been demonstrated by Kobayashi et al. [27] and the large amount of hydroxy group from PEG binding with water can enhance the hydration lubrication. Poly (ethylene glyco) bis (3-amino-propyl) terminated (PBA) is a PEG molecule with amino groups at the two ends. The amino group can be easily bioconjugated to dopamine part of HADN via Michael addition or Schiff base reactions forming loops and tails in a mild alkaline condition.

In the present study we use a facile approach for immobilizing HADN macromolecules onto PU surface followed by PBA modification of HADN. HADN was synthesized via a simple carbodiimide reaction and then attached onto PU under mild alkaline condition. Then PBA was introduced to HADN surface via Michael addition. X-ray photoelectron spectroscopy (XPS), contact angle measurements were adopt to characterized the surface properties. Furthermore, the lubrication enhancement was evaluated by universal mechanical testing machine (UMT) with PU-aorta lubrication system and the wear of aorta was evaluated as well. Besides lubrication the biocompatibility of this coating was checked and the results suggest the coating based on HADN and PBA can reduce the friction and resist wear of tissue, which benefit to cardiac catheterization application.

2. Materials and methods

Synthesis of HADN: Hyaluronic acid (Kraeber & Cogmbh, Germany) of 600 kDa was coupled to dopamine hydrochloride (Sigma, CAS no. 62-31-7) by active agent of N-(3-Dimethylaminopropyl)-N-ethylcarbodiimide hydrochloride (EDC, Sigma, CAS no.25952–53-8) as previously [28]. Briefly, 40 mg HA was dissolved in 8 mL Phosphate Buffer solution (PBS) at pH 5 adjusted by hydrochloric acid (HCl). Then 13.5 mg EDC and 19 mg dopamine were added to the HA solution at pH 5 for 5 h. The reaction was protected with nitrogen. Unreacted chemicals and byproducts were removed by extensive dialysis (molecular weight cut-off: 3500 Da, spectrum medical industries, USA) for 3 days in deionized water (pH 5) which needs to be exchanged every 3 h. Then conjugate product was lyophilized and stored at 4 °C moisture-free desiccator for further use.

Nuclear Magnetic Resonance (NMR) and Ultraviolet spectrophotometry (Uv-vis) were used to analysis of HADN. Lyophilized sample was dissolved in deuterated water at 5 mg/mL for ^{1}H NMR (Bruker Avance, 400 MHz) analyses. Dopamine solution with different concentration from 0.1 mM to 1 mM in PBS to be prepared and their spectrum absorbance at 280 nm were measured by Uv-Vis spectrum (Beckman, USA) with a cuvette of 1 cm wide. Then the standard curve was calculated by linear fitting. Once the absorbance of 1 mg/mL HADN was gotten at 280 nm the conjugate degree can be calculated.

PU surface modification with HADN and PBA: All the PU disks were cleaned with ethanol and milli-Q water. 20 mg HADN conjugate was dissolved in 5 mL PBS buffer (pH = 8, 10 mM) to a final concentration about 4 mg/mL. Then a cleaned bare PU ball was immersed in the HADN solution in room temperature overnight (37 °C, 12 h). The dipped PU was denoted as PU-HADN and washed by milli-Q water to remove the free HADN then dried in a stream of nitrogen and stored at 4 °C until used. For PU modification of HADN and PBA, 20 mg PBA (CAS no. 34901–14-9, Sigma-Aldrich Mn ~ 1500 Da) was dissolved in 5 mL and 10 mL PBS buffer (pH = 8, 10 mM) to a final concentration about 2 mg/mL and 4 mg/mL respectively. Then PU-HADN was immersed in two PBA solutions for another 12 h at room temperature, denoted as PU-HADN-PBA1 (PBA 2 mg/mL) and PU-HADN-PBA2 (4 mg/mL) washed by milli-Q water to remove the free PBA then dried in a stream of nitrogen and stored at 4 °C until used.

Surface characterization by X-ray photoelectron spectroscopy and Water contact angle: The chemical compound of the PU, PU-HADN, PU-HADN-PBA1 and PU-HADN-PBA2 were detected by XPS (S-Probe, surface science instruments, mountain view, CA, USA). XPS can only detect information within 10 nm thickness, and so it can give the very top layer information. Firstly, different PU samples were moved to XPS prevacuum chamber. Then a vacuum degree of 10^{-7} pa was applied. X-rays (10Kv, 22 mA), spot size 250 × 1000 um, were produced using an aluminum anode. Scans spectrum in binding energy range of 1-1100 eV were made at low resolution. The area with each peak can yield elemental surface concentrations for C, N, O. Correction was applied with the help of sensitivity factors provide by the manufacturer. Water contact angle measurements were performed at room temperature using an OCA 15 plus goniometer (DataPhysics Instruments). The values were obtained by the sessile drop method. The used liquid was ultrapure water and the drop volume was 5 μL. Over three measurements were carried out for each sample.

Lubrication properties of HADN-PBA on PU-blood vessel system: Polyurethane hemisphere (∅16 mm) was chosen as counterpart of aorta to mimic the materials popular for cardiovascular catheter. Sliding contact between catheter and the luminal surface of blood vessel during cardiovascular catheterization was simulated in reciprocating sliding mode on UMT-III (Bruker Corporation, American). The prepared aorta sample was placed upon the silicon rubber and fixed with pins in the specially designed bath. 8 mL PBS was add to the bath so that aorta can be immersed. The temperature of the PBS solution in bath was around 37 °C to mimic the human internal environment. According to

the suggestions of the medical practitioners as well as the previous research, the normal load was 0.6 N, and the sliding speed 6 mm/s. Friction force was measured for 40 min with a sliding distance of 30 mm per cycle using the UMT-III tribometer at a sampling rate of 20 kHz. Measured friction force was divided by the applied normal force to calculate the coefficient of friction (COF).

Glycocalyx visualization and quantification by using fluorescent microscopy: The glycocalyx on the aorta surface was observed using the Confocal laser scanning microscopy (CLSM, Leica TCS SP2 Leica, Wetzlar, Germany) with an HCX APO L40×/0.80 WU-V-1 objective. Fluorescent stain Con A (Concanavalin A, Alexa Fluor™ 488 Conjugate from ThermoFisher, Catalog no. C11252) was used to stain the glycocalyx and 6-diamidino-2-phenylindole (DAPI, CAS number 28718–90-3, Sigma-Aldrich) for the nucleus of the endothelial cells. An argon ion laser at 488 nm and a green HeNe laser at 543 nm were used to excite Con A and DAPI respectively. The fluorescent signal was collected between 500 and 540 nm for Con A and rendered green while the signal collected between 583 and 688 nm for DAPI was rendered blue. Aorta pieces were submerged in PBS and 1.5% BSA for the same amount of time as negative control. CLSM was used to take fluorescent images, where the excitation laser intensity was kept same consistently for all aorta pieces. Finally, by setting the threshold, the fluorescence intensity was calculated with the ImageJ 1.50b software (Wayne Rasband, National Institutes of Health, USA) [28,29].

Surface characterization of aorta by using scanning electron microscopy (SEM): The surface characterization of aorta before and after friction test can be visualized with scanning electron microscopy (Nova, FEI, USA). Firstly, the aorta samples were washed with PBS solution, and then fixed in 2.5% glutaraldehyde for 24 h. After the first fixation, the samples were washed with PBS solution for 3 times (10 min per time). Then the samples were immersed in 2% tannin solution twice (15 min per time) for further fixation. Thirdly, the samples were dehydrated using graded ethanol, namely immersed with alcohol with concentrations of 30%, 50%, 70%, 80%, 90%, 95% and 100% (10 min per time). Finally, the samples were placed in fume cupboard to dry for 1 h and waited for test. Due to non-conduction of biological materials, the aorta samples need spray gold craft under vacuum environment before observation.

Biocompatibility:A mouse fibroblastic cell line (L929) was used for the biocompatibility study. The coating of HADN and HADN-PBA1 and HADN-PBA2 were coated on the circular glass (15 mm ϕ) surface that fit for 24 cell culture plate and co-cultured with L929 cell line. 1×10^4 cells /well were seeded on the glass surface and cultured with high glucose DMEM (Gibco), 10% FBS (Gibco), and 1% penicillin−streptomycin (Sigma). Cells were incubated at 37 °C in a humidified air atmosphere of 5% CO_2. Cell viability was analyzed using an XTT assay [28–30] (Applichem A8088). Briefly on 1d, 3d, 7d, 14d, 300ul of XTT reaction reagent (0.1 mL activation reagent and 5 mL XTT mixture) was added to each well after incubated at 37 °C in a humidified air atmosphere of 5% CO_2 the microplate reader recorded absorbance at 485 and 690 nm.

Statistical analysis: All data are expressed as means ± SD. Differences between groups by using two-tailed Student's *t* analysis, accepting significance at $p < 0.05$.

3. Results and discussion

3.1. HADN conjugation synthesis and characterization

HADN was prepared by carbodiimide chemistry with N-(3-Dimethylaminopropyl)-N-ethylcarbodiimide hydrochloride (EDC) coupling reaction [24,25,31,32]. A schematic representation of synthetic procedure was shown in Fig. 1a. The multiplets observed between $\delta = 6.7$ ppm and $\delta = 7.0$ ppm in ^{1}H NMR spectra in Fig. 1b are associated with protons of the aromatic ring [26]. Chemical shift at 2.03 ppm is associated with protons of N-$COCH_3$ [26] demonstrating the HADN conjugation was successful. The results also were confirmed by Uv-visible spectrophotometer in Fig. 1c. An absorbance band around 280 nm, the characteristic absorbance of catechol, was observed in HADN while not shown in HA alone. Dopamine solutions with different concentration from 0.1 mM to 1 mM in PBS were prepared. Their spectrum absorbance at 280 nm were measured by Uv-Vis spectrum. Then the standard curve was calculated by linear fitting in Fig. S1. Based on a standard curve and the A_{280} nm of the synthesized product the conjugation was calculated as about 18%. Amidation by a carbodiimide coupling method [26] is widely used in biomaterial application due to features of highly effective and reproducible. Different equivalent proportion can yield different conjugation degree. In the present we chose a 18% conjugation because less than 10% is conventionally considered to be a low catechol conjugation level for polymer. Likewise, a conjugation degree over 30% is regarded to be a high catechol conjugation for polymer [33,34].

3.2. PU-HADN and PU-HADN-PBA preparation and characterization

The HADN was immobilized on PU surface via catechol groups from HADN as illustrated in schematic in Fig. 2. PU balls were immersed in the mild alkaline conditions (PBS, pH = 8) HADN with a concentration of 4 mg/mL at room temperature for 12 h enable the surface fully covered with HADN. During this period, catechol groups of HADN form quinone groups able to assist the deposition of HADN on PU surface (denoted as PU-HADN) by hydrophobic interaction [35]. PBA was grafted onto the HADN modified PU surface by dipping in two concentrations of 2 mg/mL and 4 mg/mL (denoted as PU-HADN-PBA1 and PU-HADN-PBA2 respectively) via Michael addition. To confirm surface modification was successful, XPS was adopted to detect the chemical element changes of substrate, as shown in Fig. 3b**.** On bare PU the majority element was that carbon is 78.3% and the nitrogen and oxygen 1.3% and 14.1% respectively the ratio of N/C is 1.7% (Table 1). While the relative amount of nitrogen and oxygen were increased to 5.2% and 25.7% after HADN modification with a N/C of 9.9%. This was decreased to 9.2% in HADN-PBA1 and 7.8% in HADN-PBA2 respectively. The lower ratio of N/C detected from HADN-PBA2 could be caused by higher concentration of PBA leading to more PBA coupled to HADN surface.

To characterize the wettability of PU surface modified with HADN and HADN-PBA, the static water contact angles of bare PU, PU-HADN, PU-HADN-PBA1 and PU-HADN-PBA2 surface were measured in Fig. 3. The bare PU surface was slightly hydrophobic and had a water contact angle of 91.6 ± 4.1° while it decreased to 58.6 ± 3.5°, 54.7 ± 4.7° and 54 ± 3.7° after HADN, HADN-PBA1 and HADN-PBA2 coating on the PU surface respectively. Although no significant difference between PU-HADN, PU-HADN-PBA1 and PU-HADN-PBA2, the slightly lower contact angle was observed on PU-HADN-PBA surface, which was likely attribute to the influence of PBA with strong hydration function indicating HADN-PBA is graft to PU surface successfully. Researches also have shown that a decrease in water contact angleresults from hydrophilic compound adsorption on hydrophobic surface [36], which is confirmed in our study as well.

3.3. The frictional behavior of PU-aorta interface

During the 40 min sliding, the frictional behavior between different coating showed big difference as shown in Fig. 4a. The COF between PU ball and aorta surface starts very low (~0.03) but increased gradually up to 0.17 ± 0.015 after 450 cycles of sliding, which is significant higher than PU-HADN (0.11 ± 0.001), PU-HADN-PBA1(0.07 ± 0.02) and PU-HADN-PBA2 (0.03 ± 0.01) respectively. HA is well known for high viscosity and hydration [37] that play a vital role in lubrication [38]. Catechol groups help immobilize HA to the PU surface leading to decrease of COF. The modification of PBA on HADN further decreases COF because of the lubrication property of PEG part in PBA. PBA attach to HADN surface via both amide terminals to form loops or through a single amide terminal to give rise to a tail configuration (Fig. 2) and enhance

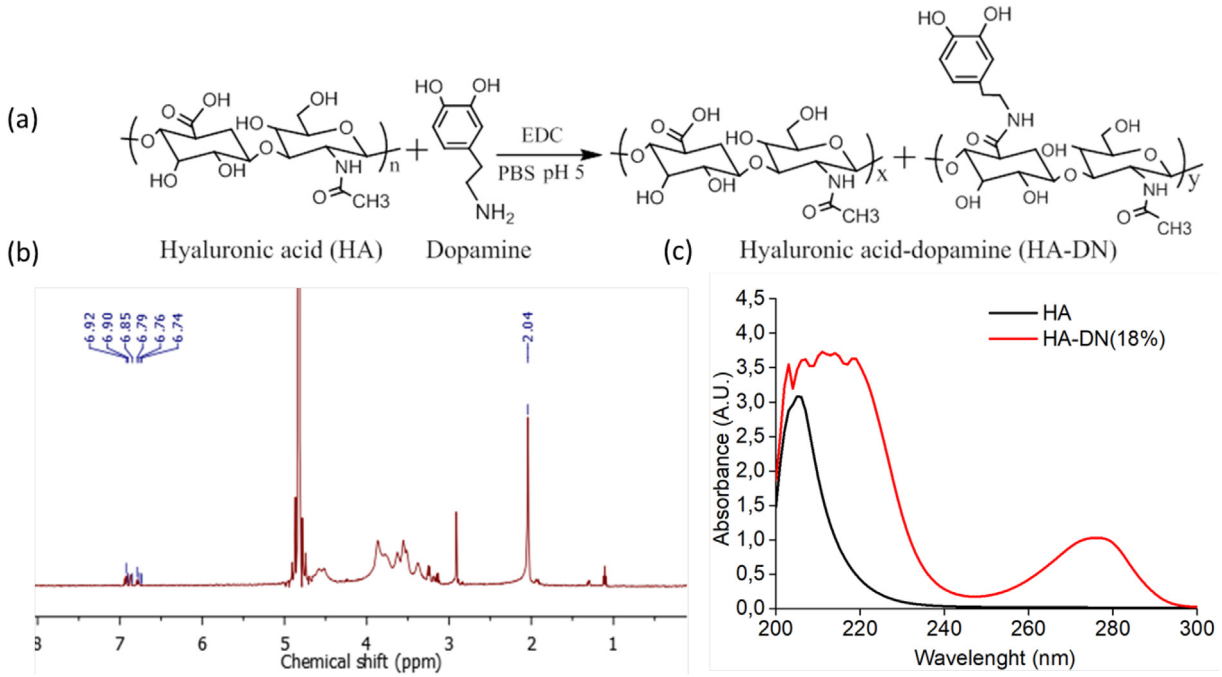

Fig. 1. Synthesis and structure of HADN. (a) is the schematic representation of procedure to synthesize HADN, b) the H-NMR specturm of HADN, UV–Vis spectra of the conjugate (HADN) and the control (HA).

lubrication. Higher concentration of PBA i.e. PU-HADN-PBA2 yield a significantly lower COF(0.03 ± 0.01) as compared to PU-HADN-PBA1 with a COF of (0.07 ± 0.02). This could be caused by higher coupling of PBA to the quinone residues of HADN. Compared to PU-HADN both PU-HADN-PBA1 and PU-HADN-PBA2 generated a lower COF which suggests the coating of PU-HADN-PBA were able to enhance the lubrication, more specifically boundary lubrication where the two surfaces are separated by a hydrated surface bound layer. The hydrated surface bound layer here is composed of HADN-PBA on the PU side and the mucinous glycocalyx on the aorta side.

Beside COF, the energy loss in the process of reciprocal sliding friction was calculated as well in Fig. 4b. It has been demonstrated that energy loss was naturally occurred in viscoelastic nonlinear materials and the loss of energy in the process of reciprocal sliding friction was positively correlated to the surface injury [39,40]. The relevant friction-displacement curve for different cycles also shows a similar tendency with COF (Fig. 4b). The energy dissipation was increased gradually between PU and aorta from 0.5 ± 0.28 mJ to 3.2 ± 0.19 mJ in 40 min i.e. 450 cycles. While the energy dissipation in group with coating were decreased dramatically after 40 min sliding, i.e., 450 cycles the energy dissipation was 1.8 ± 0.17 mJ in PU-HADN, 1.1 ± 0.46 mJ in PU-HADN-PBA1 and 0.35 ± 0.12 mJ in PU-HADN-PBA2.

In Fig. 5, the friction-displacement curve per 50 cycles shows the curve with the similar to the shape of parallelogram at each reciprocating cycle, while the area of each cycle was increased with time especially in bare PU and this was not happened in PU-HADN-PBA especially in PU-HADN-PBA2 where all the shape and area of parallelograms with time keep constant indicating the lasting lubrication property of HADN-PBA2 coating. Lower COF, lower energy dissipation and lower hydrophobicity was observed in group of PU-HADN-PBA compared to PU-HADN, which shows that all the catechol groups of HADN were not utilized for adhesion to PU but some were free to bind to the amine groups of PBA. After binding to HADN, the PEG part of PBA was able enhance the lubrication due to its hydrophilicity and higher water holding capability [27]. Although the wettability of PU-HADN-PBA2 was similar to PU-HADN-PBA1, but better lubrication of PU-

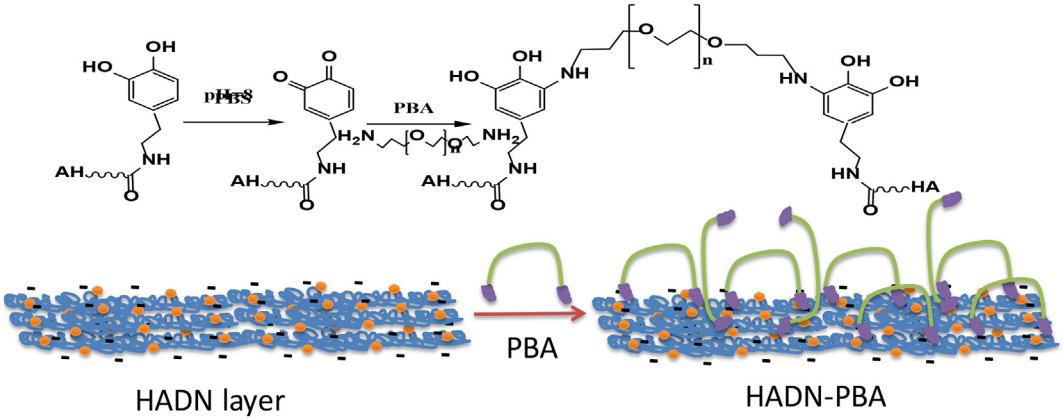

Fig. 2. Schematic illustration of HADN-PBA layer.

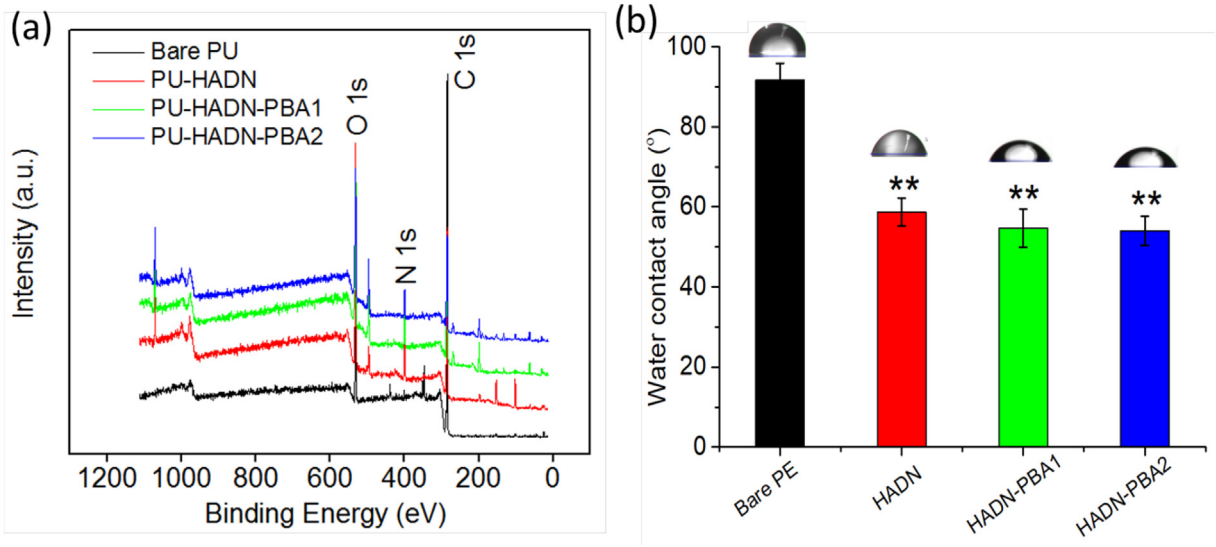

Fig. 3. Surface property of coated PU. (a) Static water contact angle of bare PU, PU-HADN, PU-HADN-PBA1 and PU-HADN-PBA2. (b) The full spectrum XPS scans, showing the chemical element of each surface. ** stands for the significance different ($p < 0.01$) of water contact angle between bare PU and PU with different coatings.

Table 1
Chemical composition of each surface.

Samples	Atomic percentages (%)			
	C	N	O	N/C
Bare PU	78.3	1.3	14.1	1.7
HADN	52.6	5.2	25.7	9.9
HADN - PBA1	53.1	4.9	28.3	9.2
HADN - PBA2	54.6	4.3	29.6	7.8

HADN-PBA2 compared to PU-HADN-PBA1 shows that either more PBA is bound to HADN or more PBA is bound as loops when HADN was exposed to higher concentration of PBA to form PU-HADN-PBA2.

3.4. The aorta luminal surface characterization, before and after friction test

Scanning electron microscopy (Fig. 6) and fluorescent microscopy (Fig. 7) was used to characterize the changes in the luminal surface and wear of aorta after sliding against different PU surfaces for 40 min and 450 cycles. The pristine aorta surface without rubbing was flat

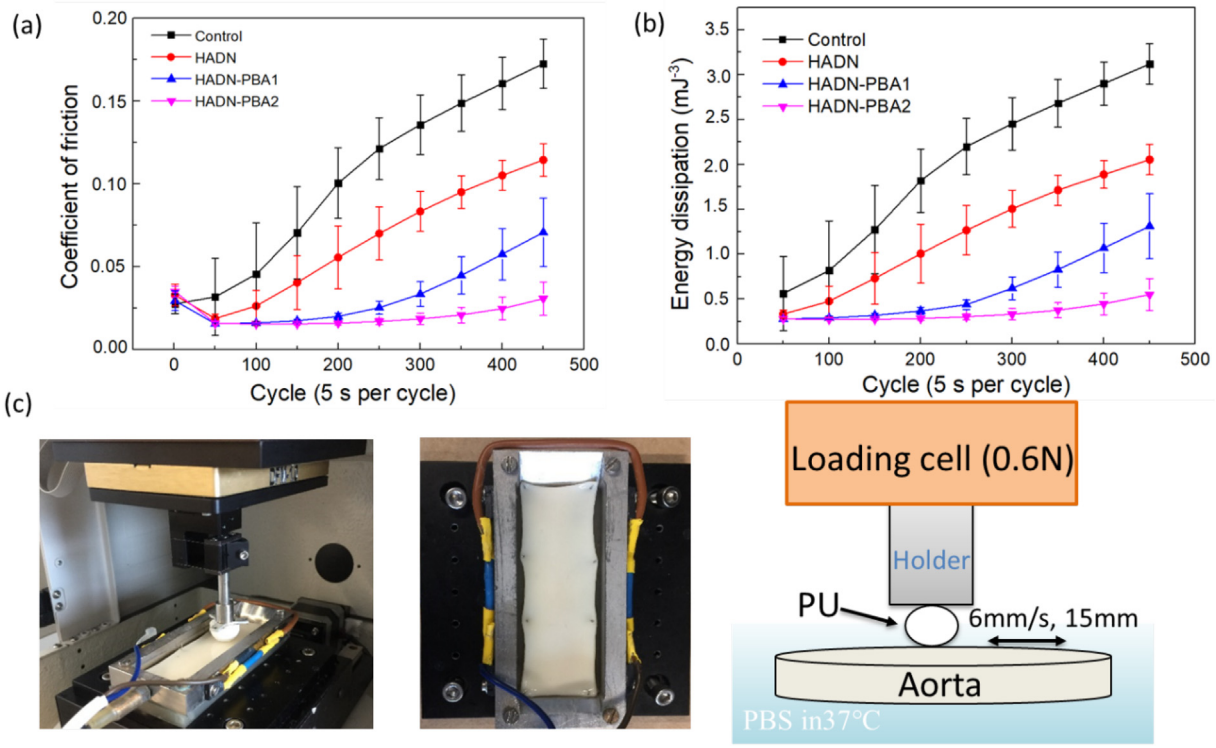

Fig. 4. Lubrication property of PU with or without (control) different coatings rubbing against aorta in PBS at 37 °C.

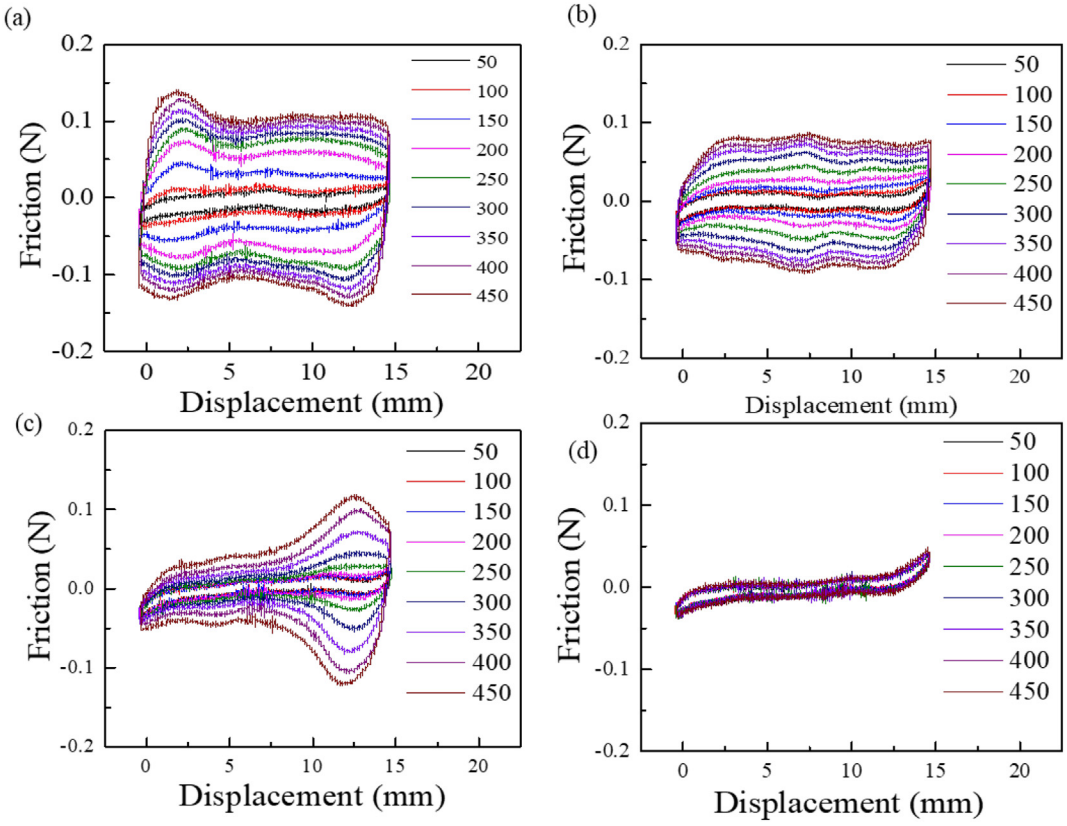

Fig. 5. The friction-displacement curves at PU-aorta interface (a) bare PU, (b) PU-HADN, (c) PU-HADN-PBA1 and (d) PU-HADN-PBA2.

and intact under the magnification from 200× to 8000× and no wear was observed on the surface with a clear texture (Fig. 6). However on the aorta surface after rubbing with bare PU ball the intima of aorta was severely damaged marked by the red circle, which might be the layer of glycocalyx. The aorta surface is composed of glycocalyx associated with the intima, media and adventitia are present deeper in the aorta wall [41]. Once the intima is gradually eliminated and the collagenous fiber and elastin gets exposed on the surface [42]. At 8000×, the exposed collagen fiber are clearly visible due to damage of the intima and rolled up glycocalyx. In contrast, in the group of coated PU especially in the PU-HADN-PBA in which no obvious damage was observed and the texture looked similar as control, where no collagenous fiber and elastin gets exposed on the surface. Thus the HADN and HADN-PBA coatings can protect the aorta surface to high degree.

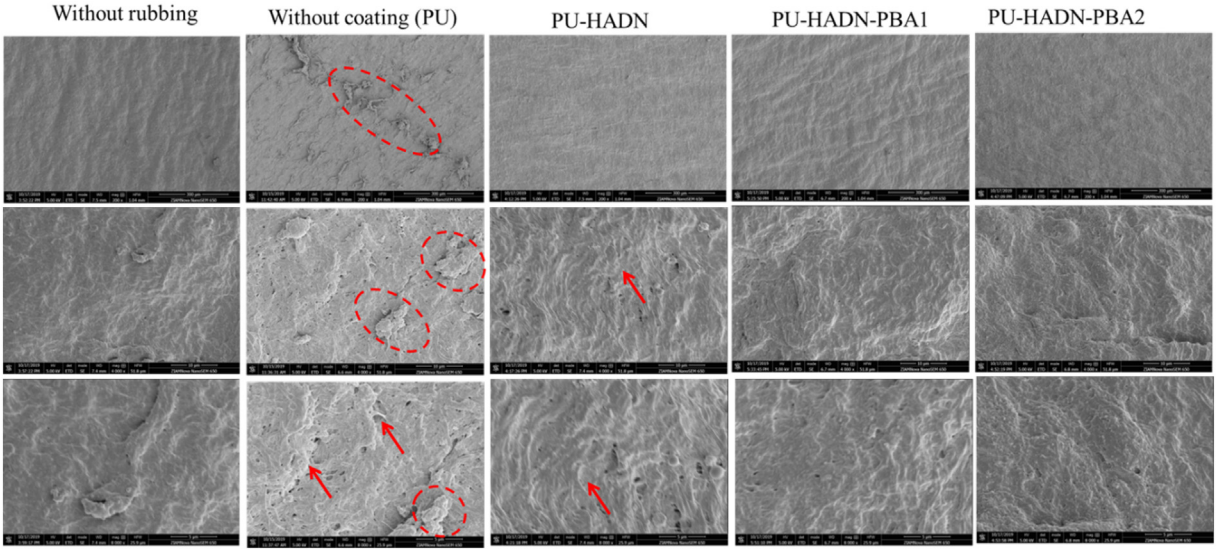

Fig. 6. The scanning electron microscopy images of aorta after rubbing against with different PU surface. The magnification from top to bottom were 200×, 4000× and 8000×. The interesting area were marked by red dotted circle and red arrow. (For interpretation of the references to colour in this figure legend, the reader is referred to the web version of this article.)

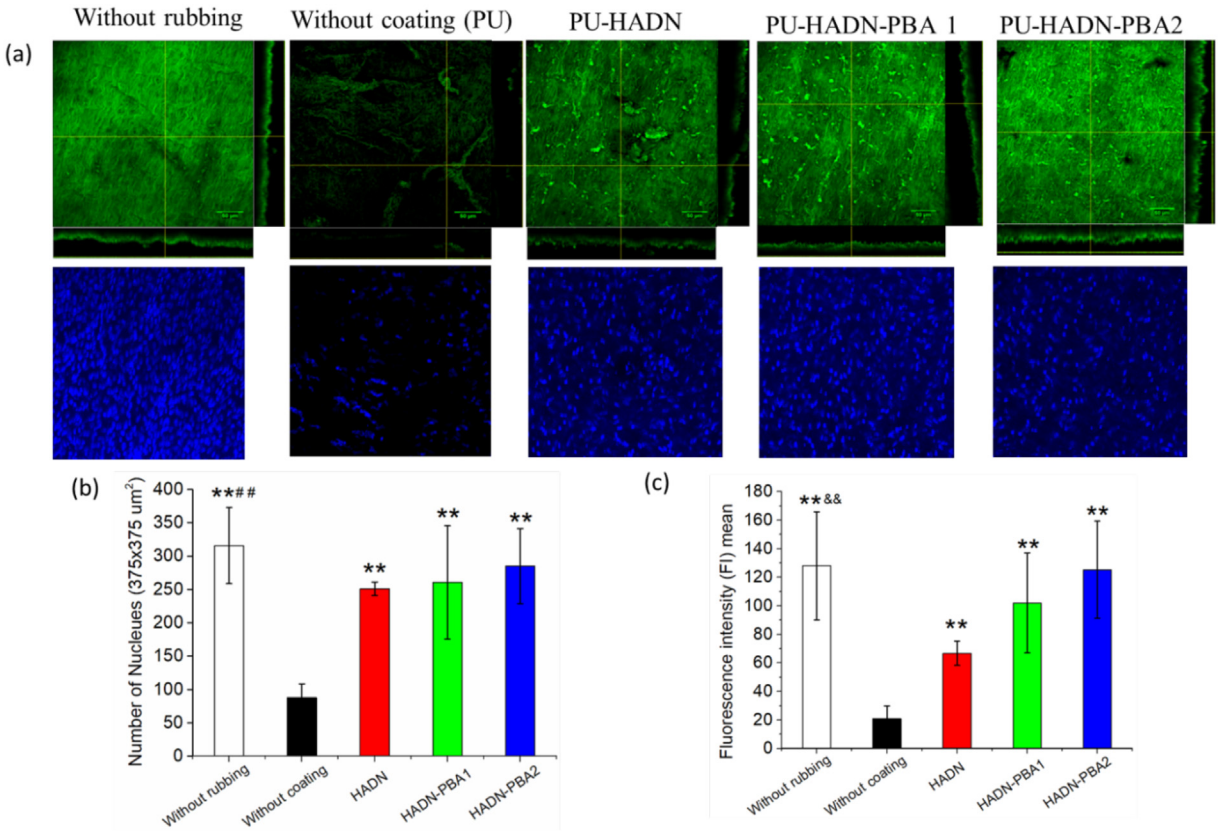

Fig. 7. The fluorescence images of aorta after rubbing against with different PU surface. The upper green fluorescence in (a) was stained by ConA for glycocalyx visualization and the blue fluorescence stained by DAPI for nucleuses visualization. (b) and (c) were the statistical results of the fluorescence and number of nucleus.** stands for the significance different ($p < 0.01$) in numbers of nucleuses and FI of aorta surface without rubbing and rubbing with coating compared to the rubbing without coating. ## stands for the significance different ($p < 0.01$) in numbers of nucleuses on aorta surface without rubbing compared to the aorta surface rubbing with coating. &&stands for the stands for the significance different ($p < 0.01$) in numbers of nucleuses on aorta surface without rubbing compared to the aorta surface rubbing with coating of HADN. (For interpretation of the references to colour in this figure legend, the reader is referred to the web version of this article.)

The degree of damage to the blood vessel lumen by HADN coated PU is greater than the coating of HADN-PBA and the latter is closer to the control group without rubbing.

The fluorescent intensity (FI) and number of nucleus of the aorta surface before and after the friction test as shown in Fig. 7. The surface of aorta without rubbing looks flat and intact and the average FI was 128 ± 38, which is significant higher ($p < 0.01$) than the aorta surface after rubbing against with bare PU ball (21 ± 8.8). Furthermore, in the side view no green signal is visible. This could be caused by the damage of intima where is fully covered with glycocalyx and once the intima is damaged or removed by the high friction the FI would be decreased. Although some damage (green aggregates) were observed on the aorta surface after rubbing against with PU-HADN, PU-HADN-PBA1 and PU-HADN-PBA2 respectively, no significant difference in FI was observed among PU, PU-HADN-PBA1 and PU-HADN-PBA2, suggesting PU-HADN-PBA can resist wear of aorta.

After sliding against bare PU the number of nucleuses decreased dramatically (Fig. 7). Sliding against coated PU causes lower decrease in the number of nucleuses compared to the bare PU.

Accompanied by the sliding process, the epithelial cells are gradually damaged. The endothelial wear seems to be so severe that the cell membranes rupture causing the cytoplasm and nucleus leaked out resulting in the decrease in the number of nucleuses in Fig. 7. These clear signs of wear on aorta surface required the catheters to be coated with suitable coating, HADN-PBA seems to be a possible solution.

3.5. Biocompatibility of HADN-PBA coating

Another important consideration for the use of HADN-PBA in vivo is the cytotoxicity. In general, coating on medical device like PU for cardiovascular catheter should be non-cytotoxic to cells [13,43,44]. In this study L292 cells were chosen for the cytotoxicity study. The coating of HADN-PBA was cocultured with L292 cells for 1, 3, 7 days and measured by XTT. The results in Fig. 8 indicated that L292 adhered on all surface well. After 3 days proliferation the cell on all surfaces shows high metabolic activity, indicating the coating is completely safe for biomedical application.

Surface coatings of the medical devices are introduced to maintain high lubrication and a low tissue wear [45,46]. Furthermore, some

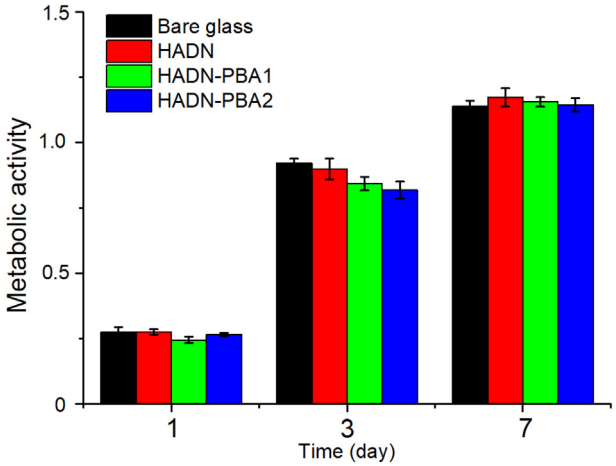

Fig. 8. Viability assay (XTT) analysis the metabolic activity of L292.

coated catheters have been tested in clinical trials such as a hydrogel- and teflon-coated catheters. Teflon-coated catheters, also known as poly (tetralfouroethanlene) coating are commercially available from Bard Medical, while their ability to reduce luminal irritation was inferior compared to the hydrogel-coated catheters [47]. Hydrogels, the swellable and hydrophilic polymer networks, contains a large amount of water on the catheter surface aim to decrease friction forces while in a clinical trial of 226 patients no difference was measured between the catheter coated with and without hydrogel [48]. Moreover, In an in vitro study, it was shown that the hydrogel coating actually increased the rate of catheter blockage [49]. Since the clinical problems associated with friction, wear and iatrogenic particle release still remain we envisage that new developments in ultra-thin coatings requires necessary attention from the surface science community and this study is thus a step in the right direction. Here, we first built an untra-thin lubricious coating based on two biocompatible biopolymers HADN and PBA, which is no risk of large particle release. High lubrication by the HADN-PBA coating maintains the luminal surface of the blood vessel intact even after 450 cycles of sliding, suggesting this coating will benefit the catheterization in the clinic.

4. Conclusion

In the study we present a polyethylene glycol functionalized hyaluronic acid based ultra-thin coating which provides excellent lubrication to the catheter surface. Superior water holding capability of polyethylene glycol loops and tails provides this excellent lubrication. This coating helps prevent any wear of the luminal surface of blood vessel for the tested 450 cycles of sliding. The coatings also shows high biocompatibility, demonstrating that the coating is safe clinical application.

Supplementary data to this article can be found online at https://doi.org/10.1016/j.matdes.2020.109080.

Author statement

HW, CL and PKS setup the study, HW synthesized the molecules, CL and HJK setup the tribological model, CL and HW performed the experiments, HW, CL and HJK analyzed the data, HW wrote the manuscript, CL, HJK, PKS critically edited and approved the manuscript.

Declaration of Competing Interest

The authors declare no competing financial interest.

Acknowledgements

The UMT-3 tribometer (Bruker) setup was purchased thanks to the grant no. 91112026 from the Netherlands Organization for Health Research and Development (ZonMW). We also would like to thank the China Scholarship Council for a 4 year scholarship to Drs. H. Wan and 1 year scholarship to Dr. Chengxiong Lin to pursue their PhD.

References

[1] D. Xie, Y.X. Leng, F.J. Jing, N. Huang, A brief review of bio-tribology in cardiovascular devices, Biosurf. Biotribol. 1 (2015) 249–262.
[2] B.D. Ratner, A.S. Hoffman, F.J. Schoen, J.E. Lemons, Biomaterials Science: An Introduction to Materials, Third edition, 2013.
[3] P. Prokopovich, S. Perni, C. Piccirillo, J. Pratten, I.P. Parkin, M. Wilson, Frictional properties of light-activated antimicrobial polymers in blood vessels, J. Mater. Sci. Mater. Med. 21 (2010) 815–821.
[4] L. Capron, P. Bruneval, Influence of applied stress on mitotic response of arteries to injury with a balloon catheter: quantitative study in rat thoracic aorta, Cardiovasc. Res. 23 (1989) 941–948.
[5] K. Takashima, R. Shimomura, T. Kitou, H. Terada, K. Yoshinaka, K. Ikeuchi, Contact and friction between catheter and blood vessel, Tribol. Int. 40 (2007) 319–328.
[6] A. Sequeira, N. Parimoo, J. Wilson, J. Traylor, S. Bonsib, K. Abreo, Polymer embolization from minimally invasive interventions, Am. J. Kidney Dis. 61 (2013) 984–987.
[7] C. FDA, Safety Alerts for Human Medical Products - Intravascular Medical Devices: FDA Safety Communication - Lubricious Coating Separation, 2015.
[8] R.W. Allan, H. Alnuaimat, W.D. Edwards, H.D. Tazelaar, Embolization of hydrophilic catheter coating to the lungs: report of a case mimicking granulomatous vasculitis, Am. J. Clin. Pathol. 132 (2009) 794–797.
[9] L.E. Rosen, R.I. Singh, B. Mahon, Myocardial hydrophilic polymer emboli following cardiac catheterization: a case report and literature review, Cardiovasc. Pathol. 23 (2014) 175–177.
[10] R.I. Mehta, R.I. Mehta, M.C. Fishbein, O.E. Solis, R. Jahan, N. Salamon, H.V. Vinters, W.H. Yong, Intravascular polymer material after coil embolization of a giant cerebral aneurysm, Hum. Pathol. 40 (2009) 1803–1807.
[11] R.I. Mehta, R.I. Mehta, O.E. Solis, R. Jahan, N. Salamon, J.M. Tobis, W.H. Yong, H.V. Vinters, M.C. Fishbein, Hydrophilic polymer emboli: an under-recognized iatrogenic cause of ischemia and infarct, Mod. Pathol. 23 (2010) 921–930.
[12] A.S.A. Hamzah, Multilayer-tuned surface plasmon modes using molecular nanolayer of (3-mercaptopropyl) trimethoxysilane applicable for nanobiosensing application, Mater. Des. 155 (2018) 99–105.
[13] W.-Z. Yu, Y. Zhang, X. Liu, Y. Xiang, Z. Li, S. Wu, Synergistic antibacterial activity of multi components in lysozyme/chitosan/silver/hydroxyapatite hybrid coating, Mater. Des. 139 (2018) 351–362.
[14] X. Li, T. Shi, B. Li, X. Chen, C. Zhang, Z. Guo, Q. Zhang, Subtractive manufacturing of stable hierarchical micro-nano structures on AA5052 sheet with enhanced water repellence and durable corrosion resistance, Mater. Des. 183 (2019) 108152.
[15] A. Berardo, G. Costagliola, S. Ghio, M. Boscardin, F. Bosia, N.M. Pugno, An experimental-numerical study of the adhesive static and dynamic friction of micro-patterned soft polymer surfaces, Mater. Des. 181 (2019) 107930.
[16] Y. Lu, H. Wang, Y. Lu, An architectural exfoliated-graphene carbon aerogel with superhydrophobicity and efficient selectivity, Mater. Des. 184 (2019) 108134.
[17] S.P. Ho, N. Nakabayashi, Y. Iwasaki, T. Boland, M. LaBerge, Frictional properties of poly(MPC-co-BMA) phospholipid polymer for catheter applications, Biomaterials. 24 (2003) 5121–5129.
[18] J. Seror, L. Zhu, R. Goldberg, A.J. Day, J. Klein, Supramolecular synergy in the boundary lubrication of synovial joints, Nat. Commun. 6 (2015) 6497.
[19] Z.M. Jin, J. Zheng, W. Li, Z.R. Zhou, Tribology of medical devices, 2 (2016) 173–192.
[20] C.C. Peng, C. Cerretani, R.J. Braun, C.J. Radke, Evaporation-driven instability of the precorneal tear film, Adv. Colloid Interf. Sci. 206 (2014) 250–264.
[21] S. Jahn, J. Seror, J. Klein, Lubrication of articular cartilage, Annu. Rev. Biomed. Eng. 18 (2016) 235–258.
[22] B. Winkeljann, K. Boettcher, B.N. Balzer, O. Lieleg, Mucin coatings prevent tissue damage at the cornea–contact Lens Interface, Adv. Mater. Interfaces 4 (2017) 1–10.
[23] B. Menchicchi, J.P. Fuenzalida, A. Hensel, M.J. Swamy, L. David, C. Rochas, F.M. Goycoolea, Biophysical analysis of the molecular interactions between polysaccharides and Mucin, Biomacromolecules. 16 (2015) 924–935.
[24] S. Hong, K. Yang, B. Kang, C. Lee, I.T. Song, E. Byun, K.I. Park, S.W. Cho, H. Lee, Hyaluronic acid catechol: a biopolymer exhibiting a pH-dependent adhesive or cohesive property for human neural stem cell engineering, Adv. Funct. Mater. 23 (2013) 1774–1780.
[25] A.I. Neto, N.L. Vasconcelos, S.M. Oliveira, D. Ruiz-Molina, J.F. Mano, High-throughput topographic, mechanical, and biological screening of multilayer films containing mussel-inspired biopolymers, Adv. Funct. Mater. 26 (2016) 2745–2755.
[26] A.I. Neto, A.C. Cibrão, C.R. Correia, R.R. Carvalho, G.M. Luz, G.G. Ferrer, G. Botelho, C. Picart, N.M. Alves, J.F. Mano, Nanostructured polymeric coatings based on chitosan and dopamine-modified hyaluronic acid for biomedical applications, Small. 10 (2014) 2459–2469.
[27] M. Kobayashi, T. Koide, S.H. Hyon, Tribological characteristics of polyethylene glycol (PEG) as a lubricant for wear resistance of ultra-high-molecular-weight polyethylene (UHMWPE) in artificial knee join, J. Mech. Behav. Biomed. Mater. 38 (2014) 33–38.
[28] H. Wan, X. Zhao, C. Lin, H.J. Kaper, P.K. Sharma, J. Accepted, Nanostructured coating for biomaterial lubrication through biomacromolecular, ACS Appl. Mater. Interfaces 12 (2020) 23726–23736.
[29] H. Wan, K. Ren, H.J. Kaper, P.K. Sharma, A bioinspired mucoadhesive restores lubrication of degraded cartilage through reestablishment of lamina splendens, Colloids Surf. B: Biointerfaces 110977 (2020).
[30] H. Wan, A. Vissink, P.K. Sharma, Enhancement in Xerostomia Patient Salivary Lubrication Using a Mucoadhesive, J. Jent. Res 99 (2020) 914–921.
[31] H. Lee, Y. Lee, A.R. Statz, J. Rho, T.G. Park, P.B. Messersmith, Substrate-independent layer-by-layer assembly by using mussel-adhesive- inspired polymers, Adv. Mater. 20 (2008) 1619–1623.
[32] W. Xu, J. Qian, G. Hou, A. Suo, Y. Wang, J. Wang, T. Sun, M. Yang, X. Wan, Y. Yao, Hyaluronic acid-functionalized gold Nanorods with pH/NIR dual-responsive drug release for synergetic targeted Photothermal chemotherapy of breast Cancer, ACS Appl. Mater. Interfaces 9 (2017) 36533–36547.
[33] A. Singh, J. Zhan, Z. Ye, J.H. Elisseeff, Modular multifunctional poly(ethylene glycol) hydrogels for stem cell differentiation, Adv. Funct. Mater. 23 (2013) 575–582.
[34] K. Kim, K. Kim, J.H. Ryu, H. Lee, Chitosan-catechol: a polymer with long-lasting mucoadhesive properties, Biomaterials. 52 (2015) 161–170.
[35] Y. Li, M. Qin, Y. Li, Y. Cao, W. Wang, Single molecule evidence for the adaptive binding of DOPA to different wet surfaces, Langmuir. 30 (2014) 4358–4366.
[36] H. Ye, Y. Xia, Z. Liu, R. Huang, R. Su, W. Qi, L. Wang, Z. He, Dopamine-assisted deposition and zwitteration of hyaluronic acid for nanoscale fabrication of low-fouling surfaces, J. Mater. Chem. B 4 (2016) 4084–4091.
[37] G.W. Greene, X. Banquy, D.W. Lee, D.D. Lowrey, J. Yu, J.N. Israelachvili, Reply to McCutchen: clarification of hydrodynamic and boundary lubrication mechanisms in joints, Proc. Natl. Acad. Sci. 108 (2011) E462.
[38] J. Seror, R. Sorkin, J. Klein, Boundary lubrication by macromolecular layers and its relevance to synovial joints, Polym. Adv. Technol. 25 (2014) 468–477.

[39] W. Li, L. Shi, H. Deng, Z. Zhou, Investigation on friction trauma of small intestine in vivo under reciprocal sliding conditions, Tribol. Lett. 55 (2014) 261–270.
[40] W. Li, Q. Pang, M. Lu, Y. Liu, Z.R. Zhou, Rehabilitation and adaptation of lower limb skin to friction trauma during friction contact, Wear. 332–333 (2015) 725–733.
[41] J. Xie, J. Zhou, Y.C. Fung, Bending of blood vessel wall: stress-strain laws of the intima-media and adventitial layers, J. Biomech. Eng. 117 (1995) 136–145.
[42] G.A. Holzapfel, T.C. Gasser, R.W. Ogden, A new constitutive framework for arterial wall mechanics and a comparative study of material models, J. Elast. 61 (2000) 1–48.
[43] Z. Li, H. Liu, X. Xu, L. Ma, S. Shang, Z. Song, Surface modification of silicone elastomer with rosin acid-based quaternary ammonium salt for antimicrobial and biocompatible properties, Mater. Des. 189 (2020) 108493.
[44] E. Frutos, M. Karlík, J.A. Jiménez, H. Langhansová, J. Lieskovská, T. Polcar, Development of new β/α ″-Ti-Nb-Zr biocompatible coating with low Young's modulus and high toughness for medical applications, Mater. Des. 142 (2018) 44–55.
[45] U. Catheters, HHS Public Access, 2018 20–40.
[46] M.J. Andersen, A.L. Flores-mireles, Urinary Catheter Coating Modifications : The Race against Catheter-Associated Infections, 2020 1–25.
[47] S. Murakami, T. Igarashi, M. Tanaka, T. Tobe, K. Mikami, Adherence of bacteria to various urethral catheters and occurrence of catheter-induced urethritis, Hinyokika Kiyo. 39 (1993) 107–111.
[48] G. Chene, G. Boulard, J.P. Gachie, A controlled trial of a new material for coating urinary catheters, Agressologie. 31 (1990) 499–501.
[49] K.A. Kazmierska, R. Thompson, N. Morris, A. Long, T. Ciach, In vitro multicompartmental bladder model for assessing blockage of urinary catheters: effect of hydrogel coating on dynamics of Proteus mirabilis growth, Urology. 76 (2010) 515–e15.